876 J. Med. Chem. 2010, 53, 876–886
DOI: 10.1021/jm900556s

Journal of Medicinal Chemistry Article

Synthesis, Radiolabeling, and Biological Evaluation of (*R*)- and (*S*)-2-Amino-3-[^{18}F]Fluoro-2-Methylpropanoic Acid (FAMP) and (*R*)- and (*S*)-3-[^{18}F]Fluoro-2-Methyl-2-*N*-(Methylamino)propanoic Acid (*N*MeFAMP) as Potential PET Radioligands for Imaging Brain Tumors

Weiping Yu,[†] Jonathan McConathy,[§,†] Larry Williams,[†] Vernon M. Camp,[†] Eugene J. Malveaux,[†] Zhaobin Zhang,[‡] Jeffrey J. Olson,[‡] and Mark M. Goodman*[,†]

[†]*Department of Radiology and* [‡]*Department of Neurosurgery , School of Medicine, Emory University, 1364 Clifton Road NE, Atlanta, Georgia 30322.* [§] *Currently at Mallinckrodt Institute of Radiology, Washington University School of Medicine, St. Louis, MO 63110.*

Received April 30, 2009

The non-natural amino acids (*R*)- and (*S*)-2-amino-3-fluoro-2-methylpropanoic acid **5** and (*R*)- and (*S*)-3-fluoro-2-methyl-2-*N*-(methylamino)propanoic acid **8** were synthesized in shorter reaction sequences than in the original report starting from enantiomerically pure (*S*)- and (*R*)-α-methyl-serine, respectively. The reaction sequence provided the cyclic sulfamidate precursors for radiosynthesis of (*R*)- and (*S*)-[^{18}F]**5** and (*R*)- and (*S*)-[^{18}F]**8** in fewer steps than in the original report. (*R*)- and (*S*)-[^{18}F]**5** and(*R*)- and (*S*)-[^{18}F]**8** were synthesized by no-carrier-added nucleophilic [^{18}F]fluorination in 52−66% decay-corrected yields with radiochemical purity over 99%. The cell assays showed that all four compounds were substrates for amino acid transport and enter 9L rat gliosarcoma cells in vitro at least in part by system A amino acid transport. The biodistribution studies demonstrated that in vivo tumor to normal brain ratios for all compounds were high with ratios of 20:1 to115:1 in rats with intracranial 9L tumors. The (*R*)-enantiomers of [^{18}F]**5** and [^{18}F]**8** demonstrated higher tumor uptake in vivo compared to the (*S*)-enantiomers.

Introduction

The development of radiotracers for tumor imaging is a major focus of radiopharmaceutical research. A number of classes of compounds that accumulate preferentially in neoplastic tissues have been investigated for this purpose, including metabolically based radiotracers such as carbohydrates, amino acids, and nucleosides. The most widely used metabolic imaging agent for oncologic applications, 2-[^{18}F]fluoro-2-deoxy-D-glucose ([^{18}F]FDG[a]), has demonstrated clinical utility in staging, treatment planning, and monitoring response to therapy for a number of types of cancers.[1,2] While [^{18}F]FDG has proven very useful, this radiopharmaceutical does have some limitations for tumor imaging including high uptake in inflammatory tissue, low or variable uptake in certain neoplasm, and high physiological uptake in certain organs and tissues, including the kidneys, urinary tract, and normal gray matter of the brain.[3,4]

Amino acids are important biological substrates in virtually all biological process and are required nutrients for cell growth,[5−7] and many tumor cells demonstrate increased amino acid transport relative to normal tissues.[8,9] Certain amino acid transporters also are involved in cell signaling and may play important roles in tumor biology.[10−12] A variety of radiolabeled amino acids have been developed as potential tumor imaging agents for positron emission tomography (PET) and single photon emission tomography (SPECT). Non-natural amino acids generally have higher metabolic stability than natural proteogenic amino acids, and this increased stability can simplify the interpretation of diagnostic images and kinetic analysis. A number of radiolabeled amino acids including tyrosine analogues *O*-(2-[^{18}F]fluoroethyl)-L-tyrosine (FET)[13] and 3-[^{123}I]iodo-α-methyl-L-tyrosine (IMT),[5,14−16] L-[^{11}C-methyl]methionine (MET)[5,17,18] and *anti*-1-amino-3-[^{18}F]-fluorocyclobutane-1-carboxylic acid (FACBC)[19] have demonstrated improved imaging properties relative to [^{18}F]FDG in human patients with gliomas.

In this study, we describe the synthesis, radiolabeling, and biological evaluation of the (*S*)- and (*R*)-enantiomers of 2-amino-3-[^{18}F]fluoro-2-methyl propanoic acid (FAMP, **5**) and 3-[^{18}F]fluoro-2-methyl-2-(methylamino)propanoic acid (*N*MeFAMP, **8**), which are fluorinated analogues of 2-amino-isobutyric acid (AIB) and 2-(methylamino)isobutryic acid (MeAIB), respectively. The major rationale for the development

*To whom correspondence should be addressed. Phone: (404) 727-9366. Fax: (404) 727-4366. E-mail: mgoodma@emory.edu.

[a] Abbreviations: ACS, alanine-cysteine-serine; AIB, 2-aminoisobutyric acid; BBB, blood−brain barrier; BCH, 2-amino-bicyclo-[2.2.1]heptane-2-carboxylic acid; Boc, *tert*-butoxycarbonyl; DMB, 4,4'-dimethoxybenzhydryl; DMEM, Dulbecco's Modified Eagle's Medium; EDTA, ethylenediaminetetraacetic acid; EOB, end of bombardment; EOS, end of synthesis; FACBC, *anti*-1-amino-3-fluorocyclobutane-1-carboxylic acid; FAMP, 2-amino-3-fluoro-2-methylpropanoic acid; FDG, 2-fluoro-2-deoxy-D-glucose; FET, *O*-(2-fluoroethyl)-L-tyrosine; HBSS, Hank's balanced salt solution; ID, injected dose; IMT, 3-iodo-α-methyl-L-tyrosine; IVAIB, 2-amino-2-methyl-4-iodo-3-(*E*)-butenoic acid; MeAIB, 2-(methylamino)isobutryic acid; MET, L-methionine; NCA, no-carrier-added; DCY, decay-corrected-yield; *N*MeFAMP, 3-fluoro-2-methyl-2-(methylamino)propanoic acid; PET, positron emission tomography; PBS, phosphate buffer solution; SPECT, single photon emission tomography.

 Published on Web 12/22/2009

of [^{18}F]FAMP and [^{18}F]*N*MeFAMP was based on preclinical results obtained with [^{11}C]AIB[20] and [^{11}C]MeAIB).[21] These compounds are primarily A-type amino acid transporter substrates, and racemic mixtures of both [^{18}F]**5** and [^{18}F]**8** have demonstrated high tumor to brain ratios in the 9L gliosarcoma rat tumor model, in part as a result of low normal brain uptake due to the absence of A-type amino acid transport across the luminal surface of normal endothelium of the blood−brain barrier (BBB).[22] Our recent comparisons of the in vitro and in vivo properties of (*S*)- and (*R*)-2-amino-2-methyl-4-[^{123}I]iodo-3-(*E*)-butenoic acid ([^{123}I]IVAIB),[23] iodovinyl substituted analogues of AIB, demonstrated that the stereochemistry of IVAIB at the α-carbon strongly affects both in vitro and in vivo properties. In the 9L gliosarcoma model, (*S*)-[^{123}I]IVAIB, an A-type amino acid transporter substrate, demonstrated superior biological properties compared to the (*R*)-enantiomer. On the basis of the above observation and the promising results obtained with racemic **5** and **8**, our goal was to improve the synthetic route and to evaluate the individual (*S*)- and (*R*)-enantiomers of **5** and **8** in the 9L gliosarcoma model to determine the effect of stereochemistry on the biological properties of these compounds.

Results and Discussion

Chemistry. The nonradioactive amino acids (*S*)- and (*R*)-**5** were prepared in a simple five-step synthesis as shown in Scheme 1. This method is an improvement over the originally reported method which employed a Strecker-type reaction to prepare compound **5** as a racemic mixture.[22] Commercially available (*S*)- and (*R*)-α-methyl-serine were treated with di-*tert*-butyl dicarbonate to give carbamates (*S*)- and (*R*)-**1**, which were used without purification in the next reaction. Because of the presence of both carboxylic acid and hydroxy functionalities, protection of the carboxylic function as a *tert*-butyl ester without ether formation was necessary. The use of *tert*-butyl-2,2,2-trichloroacetimidate led to the formation of both the *tert*-butyl ester as well as the *tert*-butyl ether. In contrast, *N*,*N*-dimethylformamide di-*tert*-butyl acetal[24,25] provided selective esterification of the carboxylic acid function when heated with (*S*)- or (*R*)-**1** in anhydrous toluene.

The next key step for making the target radiolabeling precursors (*S*)- and (*R*)-**4** was preparation of cyclic sulfamidites from **2**. The typical approach of reacting the *N*-*tert*-butoxycarbonyl (Boc) protected amino alcohols (*S*)- and (*R*)-**2** with thionyl chloride in the presence of triethylamine in low polarity solvent at low temperature failed to give the corresponding cyclic sulfamidites. Our previous strategy was to replace the Boc group with the electron releasing group bis(4-methoxyphenyl)methyl, also known as 4,4′-dimethoxybenzhydryl (DMB) group.[22] While effective, this approach added at least two synthetic steps to the sequence and required the preparation of bis(4-methoxyphenyl)chloromethane[26] for *N*-alkylation. This problem with cyclization of the *N*-Boc compound was successfully solved by utilizing Posakony's method,[27] which uses a more polar solvent for cyclization. The carbamate nitrogens of (*S*)- and (*R*)-**2** are predicted to be less nucleophilic than their *N*-alkyl counterparts, and the use of acetonitrile allowed formation of the *N*-Boc protected cyclic sulfamidites (*S*)- and (*R*)-**3**. Further oxidation of **3** using sodium periodate with ruthenium(III) chloride catalysis provided the cyclic sulfamidates (*S*)- and (*R*)-**4**, which served as radiolabeling precursors for (*R*)- and (*S*)-[^{18}F]**5**, respectively, and as intermediates for the synthesis of nonradioactive (*R*)- and (*S*)-**5** and (*R*)- and (*S*)-**8**, as well as radiolabeling precursors (*S*)- and (*R*)-**7** for (*R*)- and (*S*)-[^{18}F]**8** (Scheme 1).

The preparation of (*R*)- and (*S*)-**8** from the cyclic sulfamidate intermediates (*S*)- and (*R*)-**4**, respectively, required selective removal of the *N*-Boc group. Attempts to remove the *N*-Boc group in the presence of the *tert*-butyl ester using *p*-toluenesulfonic acid[22] or with anhydrous hydrochloric acid in dioxane[28] were not successful, presumably due to high sensitivity of the cyclic sulfamidate toward the acidic condition. Selective removal of the *N*-Boc group was achieved by treatment of **4** with methanesulfonic acid in *tert*-butyl acetate/dichloromethane as solvent.[29] The success of this reaction is likely because the removal of Boc group is an irreversible process due to protonation of the amine group and loss of CO_2. In contrast, the acidic deprotection of the *tert*-butyl ester is a reversible process due to the nature of the *tert*-butyl carbonium ion mediated equilibrium with a *tert*-Bu^+ source. The likely reaction route is displayed in Scheme 2. The possible byproducts or intermediates **9** and **10** and their interchanging between **4** and **6** were observed by TLC at different reaction points. Using a mild organic acid such as methanesulfonic acid under anhydrous condition to prevent cyclic sulfamidate ring-opening was the key to successfully prepare (*S*)- and (*R*)-**6** from (*S*)-**4** and (*R*)-**4**, respectively. The *N*-methylation of (*S*)-**6** and (*R*)-**6** was achieved by utilizing dimethyl sulfate with sodium hydride,[30] which provided (*S*)-**7** and (*R*)-**7** in good yields. Initial attempts using methyl iodide as the methylating agent for this reaction were unsuccessful.

Radiochemistry. The radiosyntheses of (*R*)-[^{18}F]**5**, (*S*)-[^{18}F]**5**, (*R*)-[^{18}F]**8**, and (*S*)-[^{18}F]**8** were carried out as shown in Scheme 3 with no-carrier-added (NCA) cyclotron-produced [^{18}F]fluoride using a modified automated method as previously described.[31] The cyclic sulfamidate precursors (*S*)-**4** and (*R*)-**4** provided an average 52 ± 12% of (*R*)-[^{18}F]**5** (n = 10) and 56 ± 12% of (*S*)-[^{18}F]**5** (n = 6) decay corrected yields (DCY), respectively, in over 99% radiochemical purity based on radiometric TLC. Similarly, treatment of (*S*)-**7** and (*R*)-**7** under the same conditions gave an average 66 ± 12% of (*R*)-[^{18}F]**8** (n = 10) and 66 ± 18% of (*S*)-[^{18}F]**8** (n = 8) DCY, respectively, in over 99% radiochemical purity. Unreacted [^{18}F]-fluoride, radiolabeled ionic byproducts as well as hydrogen chloride from the hydrolysis step were removed by passing the reaction mixture through an ion-retardation resin column followed by an alumina N Sep-Pak. Less polar and organic byproducts were removed by using a HLB Oasis reverse-phase cartridge. The purified final products (*R*)-[^{18}F]**5**, (*S*)-[^{18}F]**5**, (*R*)-[^{18}F]**8**, and (*S*)-[^{18}F]**8** were obtained in pH 6−7 normal saline solution and used directly in the cell assays and the rodent studies. In a representative synthesis, a total of 155 mCi of (*R*)-[^{18}F]**5** at end of synthesis (EOS) was obtained from 387 mCi of [^{18}F]fluoride at end of bombardment (EOB) in a synthesis time of approximately 85 min using 1 mg (3 μmol) of cyclic sulfamidate precursor (*S*)-**4**.

While the specific activities of (*R*)- and (*S*)-[^{18}F]**5** and (*R*)- and (*S*)-[^{18}F]**8** were not determined directly, the maximum amount of unlabeled material in the final product arising from the precursors is about 1 mg in each case. On the basis of a 150 mCi yield at EOS, the amount of nonradioactive material in the final dose arising from the precursor is approximately 7 μg per mCi. This amount is comparable to

Scheme 1. Syntheses of Labeling Precursors (*S*)- and (*R*)-**4** and (*S*)- and (*R*)-**7**, and Syntheses of the Fluorine-19 amino Acids (*R*)- and (*S*)-**5** and (*R*)- and (*S*)-**8**[a]

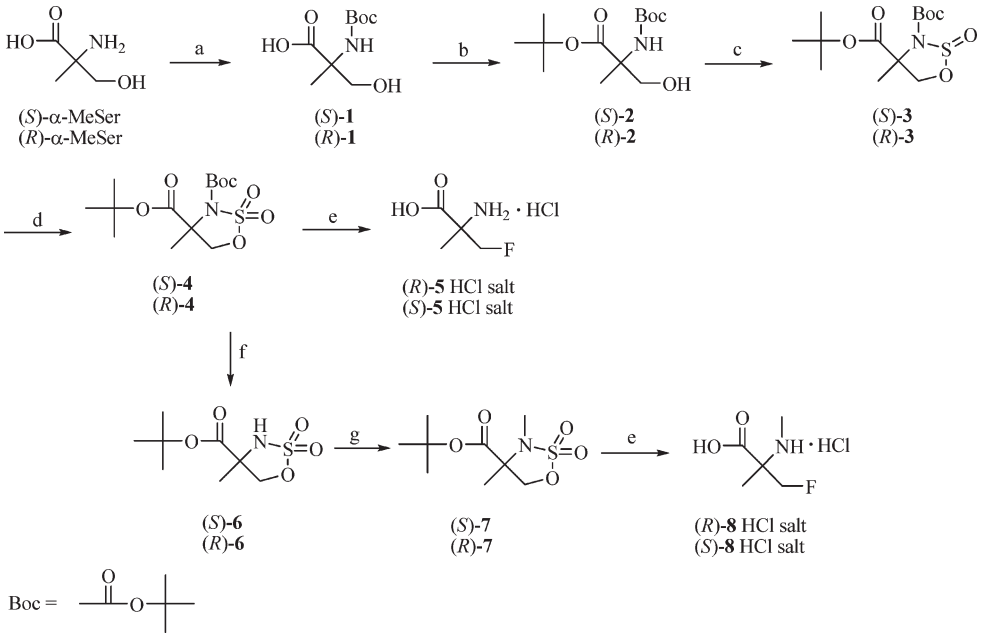

[a] Reagents and conditions: (a) $(Boc)_2O$, MeOH-Et_3N-NaOH (aq), rt. (b) $(CH_3)_2NCH[OC(CH_3)_3]_2$, 80−90 °C. (c) $SOCl_2$, Pyr, −40 °C. (d) $NaIO_4$, $RuCl_3$, CH_3CN/H_2O, 0 °C to rt. (e) *n*-Bu_4NF, rt, then 3N HCl, 85 °C. (f) $MeSO_3H$, *t*-BuOAc, DCM, rt. (g) Me_2SO_4, NaH, THF, rt.

Scheme 2. Possible Route for Deprotection of the Boc Group at the Presence of the *tert*-Butyl Ester

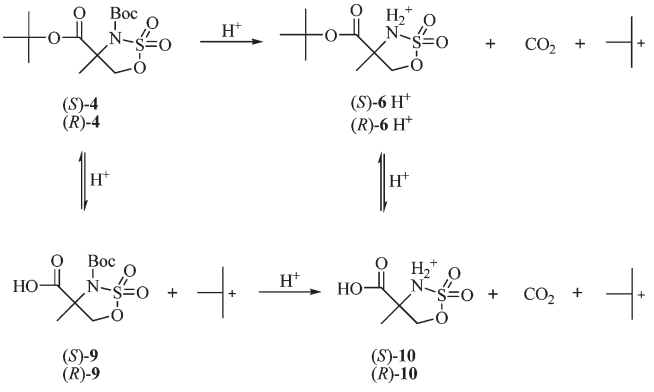

the amount of nonradioactive material present in doses of [^{18}F]FDG, which arises from the triflate precursor.[32] Similarly, the non-natural amino acid *anti*-[^{18}F]FACBC contains nonradioactive material arising from its triflate precursor.[31] On the basis of the average dosage of 5−20 μCi of [^{18}F]**5** or [^{18}F]**8** per animal in the in vivo study, the maximum amount of unlabeled material arising from the precursor associated with (*R*)- and (*S*)-[^{18}F]**5** and (*R*)- and (*S*)-[^{18}F]**8** per injection was approximately 0.034−0.13 μg. The major byproducts arising from the labeling precursor are expected to consist of α-methyl-serine or *N*-methyl-α-methyl-serine arising from opening of C-5 position of cyclic sulfamidate precursors by water or hydroxide ions.

Cell Uptake Assays. Amino acids enter normal and neoplastic cells through carrier-mediated uptake from the extracellular fluid. For radiolabeled amino acids, tumor uptake is primarily determined by amino acid transport rather than protein synthesis.[5,6] The most abundant amino acid transport systems in most mammalian cells are system A, system L, system ASC, and system Gly.[6,12,33−37] All of

Scheme 3. Radiosynthesis of (*R*)- and (*S*)-[^{18}F]**5** and (*R*)- and (*S*)-[^{18}F]**8**

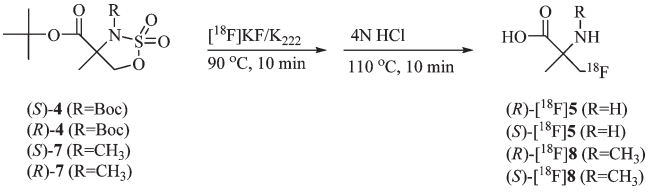

these transport systems are sodium-dependent except system L. Prior studies demonstrate that AIB and its analogues including MeAIB, (*R*,*S*)-[^{18}F]**5**, and (*R*,*S*)-[^{18}F]**8** enter cells mainly through system A transport.[20,22] To determine the transport mechanisms involved in the uptake of (*S*)- and (*R*)-[^{18}F]**5** and (*S*)- and (*R*)-[^{18}F]**8** by 9L gliosarcoma tumor cells, inhibition assays were performed using cultured rat 9L gliosarcoma cells in the presence and absence of amino acid carrier inhibitors. MeAIB is a selective competitive inhibitor of system A transport, and 2-amino-bicyclo[2.2.1]heptane-2-carboxylic acid (BCH) is an inhibitor of system L transport although it is not entirely selective for system L in the presence of sodium.[35,38,39] The combination of 10 mM alanine-cysteine-serine (ACS, 3.3 mM of each amino acid) was also used for uptake inhibition as these amino acids are substrates for system ASC. The uptake data was normalized and expressed as mean percent uptake relative to the control condition (Table 1). In all cases, ACS inhibited more than half of the uptake compared to control (58.2−90.0%). In the case of (*R*)- and (*S*)-[^{18}F]**5**, both BCH and MeAIB inhibited uptake to certain degrees, with 67−75% inhibition by BCH, and 31−58% by MeAIB. In the case of (*R*)- and (*S*)-[^{18}F]**8**, MeAIB inhibited 77−92% of uptake, whereas BCH inhibited 28−54% of uptake relative to controls (Figure 1).

On the basis of the results of these inhibition studies, (*R*)- and (*S*)-[^{18}F]**5** enter 9L gliosarcoma cells in vitro involves both system A and nonsystem A transport, likely system L.

Table 1. 9L Cell Uptake of (*R*)- and (*S*)-[^{18}F]**5** and (*R*)- and (*S*)-[^{18}F]**8** at 30 min Incubation with or without Inhibitors[a]

		control	BCH	MeAIB	ACS
(*R*)-FAMP **5**	uptake	13.06 ± 0.23	4.27 ± 0.21	5.51 ± 0.16	1.70 ± 0.02
	inhibition		67	58	87
	p		< 0.0001	< 0.0001	< 0.0001
(*S*)-FAMP **5**	uptake	4.77 ± 0.73	1.21 ± 0.13	3.29 ± 0.15	1.33 ± 0.27
	inhibition		75	31	72
	p		< 0.002	< 0.03	< 0.002
(*R*)-*N*MeFAMP **8**	uptake	7.08 ± 0.47	3.26 ± 0.22	0.60 ± 0.12	0.75 ± 0.09
	inhibition		54	92	89
	p		< 0.0001	< 0.0001	< 0.0001
(*S*)-*N*MeFAMP **8**	uptake	3.87 ± 0.22	2.76 ± 0.20	0.82 ± 0.11	1.62 ± 0.08
	inhibition		29	79	58
	p		< 0.002	< 0.0001	< 0.0001

[a] Values are reported as percent uptake of the initial dose per 0.5 million cells (% ID/5 × 10^5 cells) ± standard deviation (SD) (n = 3). Inhibition is expressed as percent relative to control (%). p values represent comparisons of uptake with inhibitors to control uptake for each radiotracer using one-way ANOVA tests.

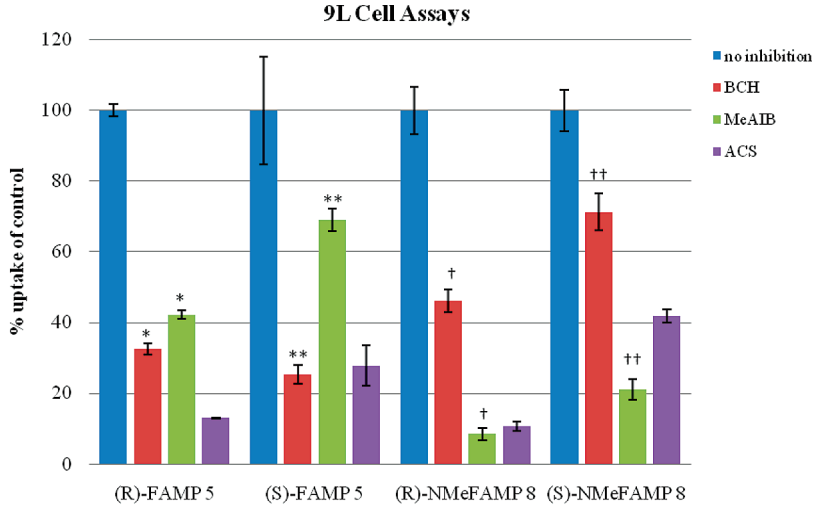

Error bars indicate ± standard deviation (n=3).
p values represent comparisons of uptake with inhibitors to control uptake for each tracer (1-way ANOVA); $p<0.03$ in all contitions.
A-type to L-type transport ratios (A/L) = %inhibition by MeAIB / %inhibition by BCH; A/L= * 0.86; ** 0.48; †1.70; †† 2.75.

Figure 1. 9L Cell percent uptake of (*R*)-[^{18}F]**5**, (*S*)-[^{18}F]**5**, (*R*)-[^{18}F]**8**, and (*S*)-[^{18}F]**8** relative to control.

(*R*)- and (*S*)-[^{18}F]**8** are relatively specific substrates for system A transport but the inhibition of uptake of these compounds in the presence of BCH, especially for (*R*)-**8**, suggests that compounds (*R*)- and (*S*)-[^{18}F]**8** entered 9L gliosarcoma cells in vitro through nonsystem A transport as well. Given the very low normal brain uptake in the biodistribution studies, it was unclear if the nonsystem A transport likely attributable to system L observed in vitro made a significant contribution to in vivo uptake.

Biodistribution Studies in Rats with Intracranial 9L Gliosarcoma Tumors. Uptake in Tumors and in Normal Brain Tissues. Prior studies using radiolabeled amino acids including racemic [^{18}F]**5** and [^{18}F]**8** in the 9L gliosarcoma tumor model demonstrated similar tissue distributions of radioactivity in tumor-bearing and normal rats.[19,22,38,39] For this reason, biodistribution was measured only in rats with intracranial tumors. The results of the tumor and normal brain uptake of (*R*)-[^{18}F] **5**, (*S*)-[^{18}F]**5**, (*R*)-[^{18}F]**8**, and (*S*)-[^{18}F]**8** are summarized in Table 2. The uptake of radioactivity by tumors was significantly higher than in normal brain tissue at each time point for all four compounds (p < 0.002). Tumor uptake of radioactivity for (*R*)-[^{18}F]**5** was 2.4−2.8% injected dose per gram of tissue (%ID/g). Under the same conditions, tumor uptake of radioactivity for (*S*)-[^{18}F]**5** was lower, in the range of 1.4−2.1%ID/g. While the uptake in normal brain contralateral tissue was similar for both [^{18}F]**5**, the ratios of tumor to normal brain uptake for (*R*)-[^{18}F]**5** was slightly higher than (*S*)-[^{18}F]**5**.

Tumor uptake of (*R*)-[^{18}F]**8** was accumulated from 1.5 to 2.8%ID/g over the time course of 120 min. Tumor uptake of (*S*)-**8** was lower and stable around 1.5%ID/g under the same conditions. The brain uptake ranged from 0.02 to 0.06%ID/g at all time points for both [^{18}F]**8**, which resulted in the tumor to brain ratios of (*R*)-[^{18}F]**8** much higher than that of (*S*)-[^{18}F]**8**.

Table 2. Uptake of Radioactivity in Tumor and Brain of Tumor-Bearing Fischer Rats Following Intravenous Administration of Radiotracers [^{18}F]**5** and [^{18}F]**8**[a]

radiotracer		15 min	30 min	60 min	120 min
(*R*)-[^{18}F]**5**	brain		0.06 ± 0.01	0.10 ± 0.02	0.09 ± 0.02
	tumor		2.46 ± 0.13	2.82 ± 0.32	2.42 ± 0.49
	tumor:brain ratio		**38.2**	**28.6**	**27.5**
(*S*)-[^{18}F]**5**	brain		0.07 ± 0.005	0.06 ± 0.005	0.08 ± 0.02
	tumor		1.38 ± 0.06	1.82 ± 0.10	2.13 ± 0.23
	tumor:brain ratio		**21.1**	**30.9**	**27.7**
(*R*)-[^{18}F]**8**	brain	0.06 ± 0.008	0.04 ± 0.01	0.05 ± 0.02	0.02 ± 0.01*
	tumor	1.46 ± 0.24	2.18 ± 0.11	2.64 ± 0.62	2.78 ± 1.13*
	tumor:brain ratio	**25.0**	**53.2**	**58.2**	**115.4**
(*S*)-[^{18}F]**8**	brain	0.06 ± 0.02	0.06 ± 0.02	0.05 ± 0.01	0.04 ± 0.01**
	tumor	1.29 ± 0.16	1.77 ± 0.32	1.46 ± 0.30	1.35 ± 0.42**
	tumor:brain ratio	**20.4**	**30.2**	**28.7**	**35.4**

[a] Values are reported as mean percent injected dose per gram tissue (%ID/g) ± standard deviation; $n = 5$ ((*R*)-[^{18}F]**5**, (*R*)-[^{18}F]**8**), and $n = 4$ ((*S*)-[^{18}F]**5**, (*S*)-[^{18}F]**8**) at each time point. *p* values were calculated using 1-way ANOVA tests (tumor vs. brain); *$p \leq 0.0006$; **$p < 0.002$; all other cases $p < 0.0001$.

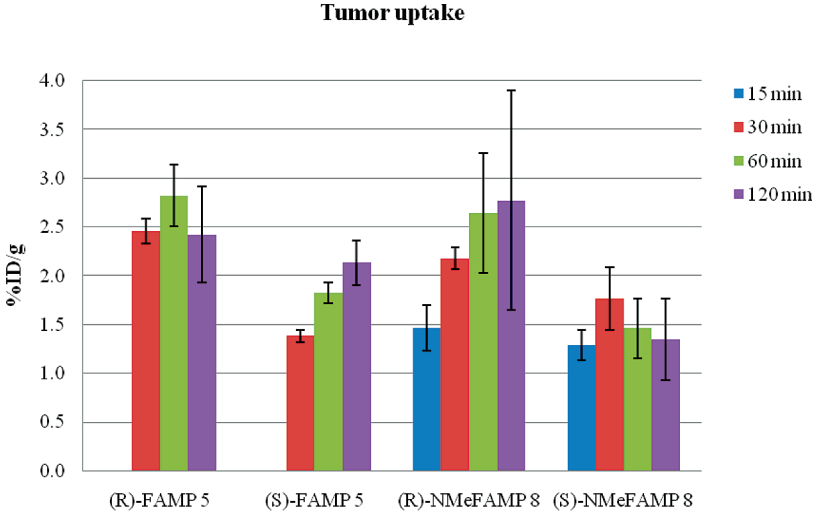

Error bars indicate ± standard deviation.
n=5, (*R*)-FAMP **5**, (*R*)-NMeFAMP **8**; n=4, (*S*)-FAMP **5**, (*S*)-NMeFAMP **8**.
p values represent the comparisons of tumor uptake (%ID/g) between tracers (1-way ANOVA).
$p \leq 0.001$, (*R*)-[^{18}F]**8** > (*S*)-[^{18}F]**5** at 30 min;
$p \leq 0.01$, (*R*)-[^{18}F]**8** > (*S*)-[^{18}F]**8** at 60 min;
$p \leq 0.02$, (*R*)-[^{18}F]**5** > (*S*)-[^{18}F]**5** at 30 and 60 min; (*R*)-[^{18}F]**5** > (*S*)-[^{18}F]**8** at all time points;
$p < 0.03$, (*R*)-[^{18}F]**5** > (*R*)-[^{18}F]**8** at 30 min; (*S*)-[^{18}F]**5** > (*S*)-[^{18}F]**8** at 120 min.

Figure 2. Comparisons of tumor uptake (%ID/g) in 9L tumor-bearing rats for (*R*)-[^{18}F]**5**, (*S*)-[^{18}F]**5**, (*R*)-[^{18}F]**8**, and (*S*)-[^{18}F]**8**.

These results in 9L gliosarcoma tumors showed that the activity accumulated to high levels in the tumors by 30 min and stayed at similar high levels through the 120 min study course for all four amino acids. The tumor uptake of these four compounds in 9L tumor-bearing rats is depicted in Figure 2. Statistically significant differences in tumor uptake were observed between the four amino acids in the biodistribution studies: (*R*)-[^{18}F]**5** > (*S*)-[^{18}F]**5** at 30 and 60 min ($p \leq 0.02$), (*R*)-[^{18}F]**5** > (*R*)-[^{18}F]**8** at 30 min ($p < 0.03$), (*R*)-[^{18}F]**5** > (*S*)-[^{18}F]**8** at all time points ($p \leq 0.02$), (*R*)-[^{18}F]**8** > (*S*)-[^{18}F]**5** at 30 min ($p \leq 0.001$), (*S*)-[^{18}F]**5** > (*S*)-[^{18}F]**8** at 120 min ($p < 0.03$), (*R*)-[^{18}F]**8** > (*S*)-[^{18}F]**8** at 60 min ($p \leq 0.01$).

The high tumor to brain ratios observed with these amino acids was in part due to the low normal brain uptake as well. The normal brain uptake of these four compounds in 9L tumor-bearing rats is presented in Figure 3. There were statistically significant differences in the levels of normal brain uptake for these amino acids at the following time points ($p < 0.04$ in all cases): (*R*)-[^{18}F]**5** > (*S*)-[^{18}F]**5** at 60 min, (*R*)-[^{18}F]**5** > (*R*)-[^{18}F]**8** at all time points, (*R*)-[^{18}F]**5** > (*S*)-[^{18}F]**8** at 60 and 120 min, (*S*)-[^{18}F]**5** > (*R*)-[^{18}F]**8** at 30 and 120 min, (*S*)-[^{18}F]**8** > (*R*)-[^{18}F]**8** at 120 min.

The tumor and brain uptake observed with (*R*)- and (*S*)-[^{18}F]**5** demonstrate that the stereochemistry of the α-carbon affects the in vivo biological behavior of these compounds. The (*R*)-enantiomer of [^{18}F]**5** demonstrated statistically significant higher tumor uptake than the (*S*)-enantiomer at the 30 and 60 min time points while the normal brain uptake with (*R*)-[^{18}F]**5** was statistically significantly

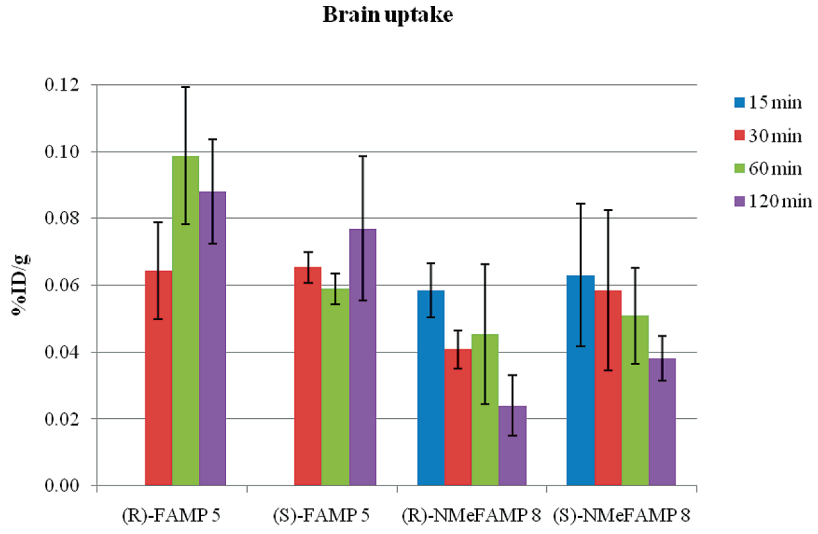

Error bars indicate ± standard deviation.
n=5, (*R*)-FAMP **5**, (*R*)-NMeFAMP **8**; n=4, (*S*)-FAMP **5**, (*S*)-NMeFAMP **8**.
p values represent the comparisons of brain uptake (%ID/g) between tracers (1-way ANOVA).
$p < 0.04$ in all cases at the following time points:
(*R*)-[^{18}F]**5** > (*S*)-[^{18}F]**5** at 60 min; (*R*)-[^{18}F]**5** > (*R*)-[^{18}F]**8** at all time points;
(*R*)-[^{18}F]**5** > (*S*)-[^{18}F]**8** at 60 and 120 min; (*S*)-[^{18}F]**5** > (*R*)-[^{18}F]**8** at 30 and 120 min;
(*S*)-[^{18}F]**8** > (*R*)-[^{18}F]**8** at 120 min.

Figure 3. Comparisons of normal brain uptake (%ID/g) in 9L tumor-bearing rats for (*R*)-[^{18}F]**5**, (*S*)-[^{18}F]**5**, (*R*)-[^{18}F]**8**, and (*S*)-[^{18}F]**8**.

higher than with (S)-enantiomer at 60 min but not at 30 or 120 min. In the case of (*R*)- and (*S*)-[^{18}F]**8**, the (*R*)-enantiomer showed statistically significant higher tumor uptake at 60 min than the (*S*)-enantiomer. The tumor uptake with (*R*)-[^{18}F]**8** at 120 min was not statistically significantly different than the (*S*)-enantiomer despite the large difference in average uptake values, which is likely due to variability in the %ID/g values at this time point. The uptake in normal brain with both enantiomers of [^{18}F]**8** was significantly different at 120 min but not at the other time points evaluated. These results are similar to (*R*)- and (*S*)-[^{123}I]IVAIB, although the difference between the enantiomers of **5** and **8** in the 9L model are not as large as for [^{123}I]IVAIB.[23]

Low brain uptake observed with all four amino acids is compatible with primarily system A transport in vivo, which is absent at the luminal surface of the endothelium of the normal BBB. The low brain uptake of (*R*)- and (*S*)-[^{18}F]**5** and (*R*)- and (*S*)-[^{18}F]**8** is consistent with the earlier studies performed with [^{11}C]AIB[20] as well as racemic [^{18}F]**5** and [^{18}F]**8**.[22] The in vitro inhibition of uptake of these compounds by BCH indicates nonsystem A transport and is compatible with a component of system L transport. Because system L transport occurs across the normal BBB, substrates for system L would be expected to show uptake in normal brain. The in vitro assay conditions were performed in the absence of amino acids, and it is possible that endogenous system L substrates competitively inhibit the transport of (*R*)- and (*S*)-[^{18}F]**5** and (*R*)- and (*S*)-[^{18}F]**8** in vivo. Future imaging studies in nonhuman primates and in human cancer patients will provide more detailed information regarding the biodistribution and kinetics of tracers in normal and neoplastic tissues.

For all four compounds studied, the tumor to brain ratios are higher than those reported for [^{18}F]FDG and *anti*-[^{18}F]FACBC in the same 9L gliosarcoma tumor model and similar to the results obtained with the racemic mixtures of [^{18}F]**5** and [^{18}F]**8**.[19,22] The activity uptake of [^{18}F]FDG at 60 min post injection was 1.05%ID/g in tumor and 1.30%ID/g in normal brain, giving a tumor to brain ratio of 0.8:1. This low ratio is consistent with the high physiologic uptake of [^{18}F]FDG in normal brain tissue. For *anti*-[^{18}F]FACBC, the uptake ratio of tumor to brain at 60 min post injection was 6.6:1, with 1.72%ID/g in tumor and 0.26%ID/g in brain tissue. The higher tumor to brain ratios observed with (*R*)-[^{18}F]**8** and (*R*)- and (*S*)-[^{18}F]**5** compared to [^{18}F]FDG and *anti*-[^{18}F]FACBC were due to a combination of higher levels of tumor uptake of tracer and much lower uptake in normal brain. The higher tumor to brain ratio of compound (*S*)-[^{18}F]**8** compared to [^{18}F]FDG and *anti*-[^{18}F]FACBC is due to the lower normal brain uptake.

Table 3. Biodistribution of Radioactivity in Tissues (Other than Tumor and Brain) of Tumor-Bearing Fischer Rats Following Intravenous Administration of (*R*)-[^{18}F]**5**[a]

tissue	30 min	60 min	120 min
blood	0.28 ± 0.03	0.25 ± 0.01	0.16 ± 0.03
heart	0.32 ± 0.05	0.34 ± 0.05	0.23 ± 0.04
lung	0.37 ± 0.08	0.40 ± 0.03	0.23 ± 0.03
liver	0.60 ± 0.06	0.65 ± 0.11	0.32 ± 0.07
pancreas	2.96 ± 0.52	2.05 ± 0.47	1.17 ± 0.17
spleen	0.72 ± 0.07	0.71 ± 0.07	0.39 ± 0.05
kidney	3.47 ± 0.69	2.96 ± 0.46	2.09 ± 0.20
muscle	0.32 ± 0.05	0.52 ± 0.07	0.36 ± 0.09
bone	0.23 ± 0.10	0.36 ± 0.12	0.26 ± 0.02
testis	0.15 ± 0.02	0.17 ± 0.01	0.16 ± 0.03

[a] Values are reported as mean percent injected dose per gram tissue (%ID/g) ± standard deviation; $n = 5$ at each time point.

Uptake in Normal Tissues. The results of the biodistribution studies with (*R*)- and (*S*)-[^{18}F]**5** in normal tissues of tumor-bearing rats are shown in Tables 3 and 4. The organs which received highest radioactivity were kidneys and pancreas ($p < 0.0001$ compared to other tissues studied), with (*S*)-[^{18}F]**5** higher than (*R*)-[^{18}F]**5** at all time points. The activity in these tissues remained above the activity in other

Table 4. Biodistribution of Radioactivity in Tissues (Other than Tumor and Brain) of Tumor-Bearing Fischer Rats Following Intravenous Administration of (*S*)-[^{18}F]**5**[a]

tissue	30 min	60 min	120 min
blood	0.58 ± 0.04	0.40 ± 0.03	0.32 ± 0.04
heart	0.43 ± 0.05	0.41 ± 0.06	0.34 ± 0.02
lung	0.67 ± 0.09	0.47 ± 0.07	0.36 ± 0.02
liver	0.61 ± 0.07	0.54 ± 0.07	0.42 ± 0.04
pancreas	3.75 ± 0.66	3.91 ± 0.49	2.79 ± 0.49
spleen	0.73 ± 0.07	0.62 ± 0.04	0.51 ± 0.02
kidney	8.71 ± 0.76	7.62 ± 0.39	6.88 ± 0.83
muscle	0.47 ± 0.02	0.37 ± 0.03	0.36 ± 0.06
bone	0.30 ± 0.09	0.30 ± 0.04	0.31 ± 0.02
testis	0.19 ± 0.02	0.16 ± 0.01	0.17 ± 0.01

[a] Values are reported as mean percent injected dose per gram tissue (%ID/g) ± standard deviation; $n = 4$ at each time point.

Table 5. Biodistribution of Radioactivity in Tissues (Other than Tumor and Brain) of Tumor-Bearing Fischer Rats Following Intravenous Administration of (*R*)-[^{18}F]**8**[a]

tissue	15 min	30 min	60 min	120 min
blood	0.41 ± 0.03	0.32 ± 0.04	0.24 ± 0.08	0.14 ± 0.04
heart	0.55 ± 0.14	0.23 ± 0.02	0.24 ± 0.08	0.22 ± 0.01
lung	0.79 ± 0.28	0.36 ± 0.02	0.38 ± 0.19	0.25 ± 0.06
liver	0.60 ± 0.12	0.61 ± 0.11	0.52 ± 0.07	0.40 ± 0.09
pancreas	2.25 ± 1.16	2.72 ± 0.62	3.41 ± 0.48	3.39 ± 0.79
spleen	0.57 ± 0.06	0.63 ± 0.06	0.59 ± 0.11	0.62 ± 0.09
kidney	9.22 ± 1.26	8.91 ± 1.32	4.44 ± 0.89	2.45 ± 1.10
muscle	0.27 ± 0.07	0.23 ± 0.03	0.20 ± 0.02	0.22 ± 0.03
bone	0.51 ± 0.09	0.48 ± 0.08	0.51 ± 0.08	0.44 ± 0.13
testis	0.19 ± 0.07	0.15 ± 0.01	0.15 ± 0.06	0.16 ± 0.06

[a] Values are reported as mean percent injected dose per gram tissue (%ID/g) ± standard deviation; $n = 5$ at each time point.

tissues ($p \leq 0.0003$ at all time points). For (*R*)-[^{18}F]**5**, the radioactivity uptake in kidneys and pancreas were 3.5 and 3.0%ID/g at 30 min post injection, respectively, which decreased to 2.1 and 1.2%ID/g at 120 min post injection, respectively. In the case of (*S*)-[^{18}F]**5**, the uptake of activity in these tissues were 8.7 and 3.8%ID/g at 30 min post injection, respectively, which decreased to 6.9 and 2.8%ID/g at 120 min post injection, respectively. With both enantiomers of [^{18}F]**5**, the tissues studied including blood, liver, heart, lung, spleen, bone, muscle, and testis showed relatively low uptake of radioactivity at 30 min (≤0.73% ID/g) which decreased over the course of the two hour study. The brain showed the lowest uptake of radioactivity for both enantiomers of [^{18}F]**5** with less than 0.1%ID/g at all time points ($p \leq 0.0001$ compared to other tissues studied).

For (*R*)- and (*S*)-[^{18}F]**8**, the pattern of biodistribution in normal tissues of tumor-bearing rats was similar to that of (*R*)- and (*S*)-[^{18}F]FAMP **5**. These results are depicted in Tables 5 and 6. For both enantiomers of [^{18}F]**8**, the highest radioactivity uptake occurred in kidneys ($p < 0.0001$ compared to other tissues studied), which decreased through the course of study from 9.2%ID/g at 15 min post injection to 2.5%ID/g at 120 min post injection for (*R*)-[^{18}F]**8** and from 11.6%ID/g at 15 min post injection to 2.2%ID/g at 120 min post injection for (*S*)-[^{18}F]**8**. The second highest radioactivity uptake was found in the pancreas ($p < 0.0001$ compared to other tissues studied), which stayed at the same level through the time course of the study with the average value of 2.9 and 3.8%ID/g for (*R*)-[^{18}F]**8** and (*S*)-[^{18}F]**8**, respectively. Similar to [^{18}F]**5**, both enantiomers of [^{18}F]**8** showed relatively low uptake in the other organs and tissues, and the lowest activity

Table 6. Biodistribution of Radioactivity in Tissues (Other than Tumor and Brain) of Tumor-Bearing Fischer Rats Following Intravenous Administration of (*S*)-[^{18}F]**8**[a]

tissue	15 min	30 min	60 min	120 min
blood	0.54 ± 0.02	0.31 ± 0.03	0.24 ± 0.02	0.14 ± 0.01
heart	0.32 ± 0.02	0.30 ± 0.06	0.31 ± 0.04	0.21 ± 0.03
lung	0.86 ± 0.10	0.87 ± 0.20	0.50 ± 0.05	0.42 ± 0.16
liver	0.83 ± 0.06	0.71 ± 0.01	0.88 ± 0.29	0.60 ± 0.12
pancreas	3.52 ± 1.15	3.40 ± 0.38	4.34 ± 1.13	3.78 ± 0.39
spleen	0.57 ± 0.10	0.51 ± 0.05	0.53 ± 0.06	0.49 ± 0.05
kidney	11.58 ± 1.88	9.48 ± 2.48	5.18 ± 0.56	2.22 ± 0.16
muscle	0.25 ± 0.02	0.26 ± 0.07	0.24 ± 0.03	0.22 ± 0.03
bone	0.46 ± 0.07	0.32 ± 0.07	0.37 ± 0.03	0.25 ± 0.06
testis	0.19 ± 0.01	0.13 ± 0.01	0.13 ± 0.03	0.08 ± 0.01

[a] Values are reported as mean percent injected dose per gram tissue (%ID/g) ± standard deviation; $n = 4$ at each time point.

uptake in brain of less than 0.07%ID/g at all time points ($p < 0.0001$ compared to other tissues studied).

The high pancreatic and renal uptake in rodent models has been reported for numerous radiolabeled amino acids including substrates for system L and system A.[21−23,38−47] The lack of significant accumulation of radioactivity in bone indicates that significant in vivo defluorination resulting from metabolism did not occur with either of these compounds during the two hour studies. Overall, the (*R*)-enantiomers of **5** and **8** have better imaging properties in the 9L model than the corresponding (*S*)-enantiomers with lower uptake in the kidneys and pancreas. This difference may be due to the similarity of the α-carbon stereochemistry of (*R*)-[^{18}F]**5** and (*R*)-[^{18}F]**8** to the naturally occurring amino acids (*S*)-serine and (*S*)-alanine.

Conclusions

The current study demonstrates that (*R*)- and (*S*)-[^{18}F]**5** and (*R*)- and (*S*)-[^{18}F]**8** can be produced in high radiochemical yield (>52% DCY) and high radiochemical purity from stable precursors using a semiautomated synthesis system. Additionally, a new synthetic strategy provides a more efficient route to enantiomerically pure radiolabeling precursors. We found that the stereochemistry influenced the uptake of these compounds by 9L gliosarcoma cells. The inhibition experiments showed that (*R*)- and (*S*)-[^{18}F]**5** entered 9L tumor cells in vitro via mixed system A and system L amino acid transport, with more L-type propensity for (*S*)-[^{18}F]**5**. Both (*S*)- and (*R*)-[^{18}F]**8** enter 9L cells in vitro primarily via system A transport. Biodistribution studies with all four amino acids demonstrated rapid and persistent retention of radioactivity in rodent brain tumors with excellent tumor to background ratios of 20:1 to115:1. The stereochemistry at the α-carbon influenced the in vivo behavior of these compounds, with the (*R*)-enantiomers of [^{18}F]**5** and [^{18}F]**8** leading to significantly higher tumor uptake than the corresponding (*S*)-enantiomers at several time points. The relatively low uptake of radioactivity of these compounds in most normal tissues with the exception of the kidney and pancreas suggests that these compounds might be suitable for imaging extracranial tumors as well.

Experimental Section

Materials and Instrumentation. All chemicals used were obtained from commercially available sources, were of analytical or higher grade, and were used without further purification. Solvents used in reactions and purifications were purchased

from Aldrich Chemicals Co. (Milwaukee, WI) and from VWR Scientific Products (West Chester, PA). Thin-layer chromatography (TLC) analyses were performed with 250 μm thick layers of fluorescence UV254 silica gel backing on aluminum plates purchased from Whatman Ltd. (Maidstone, Kent, England). Flash chromatography was carried out using Merck Kieselgel silica gel 60 (230−400 mesh). Melting points were measured in capillary tubes using a Mel-Temp II apparatus (Laboratory Devices, Inc., Holliston, MA) and are uncorrected. ^{1}H NMR spectra were recorded on Varian 600, 400, or 300 MHz spectrometers at NMR Center in Emory University, and chemical shifts (δ values) were reported as parts per million (ppm) downfield from tetramethylsilane (TMS). Elemental analyses were performed by Atlantic Microlabs, Inc. (Norcross, GA) and were within ±0.4% of the theoretical values unless otherwise indicated. A few of the products were oils which contained trace amounts of solvents and were characterized by high resolution mass spectrometry in conjunction with NMR and TLC to confirm identity. In each and every case, the purity of the identified compound was greater than 95%. Mass spectrometry was performed with a JEOL JMS-SX102/SX102A/E or VG 70-S double focusing mass spectrometer at the Mass Spectrometry Center at Emory University using high resolution electrospray ionization (ESI). Observed masses were within 9 ppm of calculated values.

The [^{18}F]fluoride used for radiosyntheses was produced at Emory University with a 11 MeV Siemens RDS 112 negative-ion cyclotron (Knoxville, TN) by the ^{18}O (p,n) ^{18}F reaction using [^{18}O]H_2O (95%). Trap/release cartridges model DW-TRC were purchased from D&W, Inc. (Oakdale, TN). Alumina N SepPak and HLB Oasis reverse phase cartridge were purchased from Waters, Inc. (Milford, MA). Ion-retardation resin (AG 11A8 50−100 mesh) was purchased from BioRad (Hercules, CA). The 0.2 μm Gelman Teflon filters were purchased from VWR. Isolated radiochemical yields were determined using a dose-calibrator (Capintec CRC-712M). Thin layer chromatograms of the radiolabeled compounds were analyzed with a Raytest System (model: Rita Star, Germany) using the same type of TLC plates from Whatman.

All animal experiments were carried out under humane conditions and were approved by the Institutional Animal Use and Care Committee (IUCAC) and Radiation Safety Committees at Emory University.

Chemistry. (*S*)- and (*R*)-2-*N*-(*tert*-Butoxycarbonyl)amino-2-methyl-3-hydroxy-propanoic Acid (1). (*S*)-(+)-2-Amino-2-methyl-3-hydroxy-propanoic acid or (*R*)-(−)-2-amino-2-methyl-3-hydroxy-propanoic acid [(*S*)- or (*R*)-α-methyl-serine] (773 mg, 6.48 mmol, Acros Organics, Morris Plains, NJ) was suspended in 20 mL methanol-triethylamine-1N sodium hydroxide (9:1:1 v/v/v) and di-*tert*-butyl dicarbonate (2828 mg, 12.96 mmol) was added in one portion. The reaction was stirred at room temperature overnight. The organic solvent was removed under reduced pressure, and 10 mL of ethyl acetate was added. The pH of the aqueous phase was adjusted to 2 with 3N hydrochloric acid. The organic layer was retained while the aqueous layer was saturated with sodium chloride and extracted with ethyl acetate (3 × 10 mL). The combined organic phases were dried over magnesium sulfate, filtered, and concentrated to dryness under reduced pressure. The product (*S*)- or (*R*)-**1** was given as white solid, which were used without further purification. (*S*)-2-*N*-(*tert*-Butoxycarbonyl)amino-2-methyl-3-hydroxy-propanoic acid ((*S*)-**1**), 1185 mg (83.5%), mp 114−117 °C (decomposed). ^{1}H NMR ($CDCl_3$) δ 1.47 (9H, s), 1.52 (3H, s), 3.79, 3.82 (1H, d, J = 12 Hz), 3.93, 3.96 (1H, d, J = 12 Hz), 5.51 (1H, broad s). (*R*)-2-*N*-(*tert*-butoxycarbonyl)amino-2-methyl-3-hydroxy-propanoic acid ((*R*)-**1**), 1400 mg (quantitative), mp 115−117 °C (decomposed). ^{1}H NMR ($CDCl_3$) δ 1.46 (9H, s), 1.51 (3H, s), 3.81, 3.84 (1H, d, J = 12 Hz), 3.91, 3.94 (1H, d, J = 12 Hz), 5.50 (1H, broad s).

(*S*)- and (*R*)-2-*N*-(*tert*-Butoxycarbonyl)amino-2-methyl-3-hydroxy-propanoic Acid *tert*-Butyl Ester (2). To a suspension of (*S*)- or (*R*)-**1** (595 mg, 2.72 mmol) in 15 mL dry toluene was added *N*,*N*-dimethylformamide di-*tert*-butyl acetal (2762 mg, 13.9 mmol) over 10 min at room temperature under an argon atmosphere. The mixture was heated to reflux at 80−90 °C for 2 h and then at room temperature overnight. The reaction was washed with water (1 × 8 mL), saturated sodium bicarbonate (1 × 5 mL), and brine (1 × 10 mL) successively. After drying over sodium sulfate, the solvent was removed under reduced pressure. The crude product was purified by flash chromatography (20% ethyl acetate in hexane) to give (*S*)- or (*R*)-**2** as white solid. (*S*)-**2**-*N*-(*tert*-Butoxycarbonyl)amino-2-methyl-3-hydroxy-propanoic acid *tert*-butyl ester ((*S*)-**2**), 267 mg (35.7%), mp 72−74 °C (ethyl acetate/hexane). ^{1}H NMR ($CDCl_3$) δ 1.435 (3H, s), 1.440 (9H, s), 1.475 (9H, s), 3.249 (1H, broad s), 3.707, 3.735 (1H, d, J = 11.2 Hz), 3.986, 4.014 (1H, d, J = 11.2 Hz), 5.32 (1H, broad s). Anal. ($C_{13}H_{25}NO_5$) C, H, N. (*R*)-2-*N*-(*tert*-butoxycarbonyl)amino-2-methyl-3-hydroxy-propanoic acid *tert*-butyl ester ((*R*)-**2**), 290 mg (38.9%), mp 72−74 °C (ethyl acetate/hexane). ^{1}H NMR ($CDCl_3$) δ 1.44 (3H, s), 1.45 (9H, s), 1.48 (9H, s), 3.71, 3.74 (1H, d, J = 11.4 Hz), 3.98, 4.02 (1H, d, J = 11.4 Hz), 5.33 (1H, broad s). Anal. ($C_{13}H_{25}NO_5$) C, H, N.

(*S*)- and (*R*)-3-(*tert*-Butoxycarbonyl)-4-methyl-1,2,3-oxathiazolidine-4-carboxylic Acid *tert*-butyl Ester 2-Oxide (3). To a solution of thionyl chloride (297 mg, 2.5 mmol) in 4 mL of anhydrous acetonitrile cooled to −40 °C was added the amino alcohol (*S*)- or (*R*)-**2** (275 mg, 1.0 mmol) in 1 mL of anhydrous acetonitrile under an argon atmosphere followed by the addition of pyridine (396 mg, 5 mmol). After 15 min, the cold bath was removed, and the reaction was continued for 10 min. The solvent was removed under reduced pressure. The crude product was subjected to silica gel column chromatography (20% ethyl acetate in hexane) to afford a ~1.2:1 mixture of cyclic sulfamidite diastereomers (*S*)- or (*R*)-**3** as colorless oil. The purified mixture of sulfamidite diastereomers was used in the next step reaction without separation. (*S*)-3-(*tert*-Butoxycarbonyl)-4-methyl-1,2,3-oxathiazolidine-4-carboxylic acid *tert*-butyl ester 2-oxide ((*S*)-**3**), 306 mg (95.3%). ^{1}H NMR ($CDCl_3$) for major diastereomer: δ 1.49 (9H, s), 1.54 (9H, s), 1.59 (3H, s), 4.57 (1H, d, J = 8.8 Hz), 4.74 (1H, d, J = 8.8 Hz). ^{1}H NMR ($CDCl_3$) for minor diastereomer: δ 1.49 (9H, s), 1.55 (9H, s), 1.61 (3H, s), 4.44 (1H, d, J = 8.0 Hz), 5.10 (1H, d, J = 8.0 Hz). Anal. for mixture of diastereomers ($C_{13}H_{23}NO_6S$), C, H, N. (*R*)-3-(*tert*-Butoxycarbonyl)-4-methyl-1,2,3-oxathiazolidine-4-carboxylic acid *tert*-butyl ester 2-oxide ((*R*)-**3**), 216 mg (67.2%). ^{1}H NMR ($CDCl_3$) for major diastereomer: δ 1.47 (9H, s), 1.53 (9H, s), 1.59 (3H, s), 4.55 (1H, d, J = 9.2 Hz), 4.73 (1H, d, J = 8.8 Hz). ^{1}H NMR ($CDCl_3$) for minor diastereomer: δ 1.49 (9H, s), 1.55 (9H, s), 1.60 (3H, s), 4.43, 4.45 (1H, d, J = 8.0 Hz), 5.09, 5.11 (1H, d, J = 8.0 Hz). Anal. for mixture of diastereomers ($C_{13}H_{23}NO_6S$), C, H, N.

(*S*)- and (*R*)-3-(*tert*-Butoxycarbonyl)-4-methyl-1,2,3-oxathiazolidine-4-carboxylic Acid *tert*-Butyl Ester 2,2-Dioxide (4). A solution of the diastereomeric sulfamidites (*S*)- or (*R*)-**3** (154 mg, 0.48 mmol) in 6 mL of acetonitrile was cooled to 0 °C and treated successively with a catalytic portion of $RuCl_3$ (2 mg, 0.01 mmol) and sodium periodate (123 mg, 0.58 mmol). The reaction mixture was then treated with 6 mL of water and stirred at 0 °C for 15 min and then at room temperature overnight. Following dilution of the reaction mixture with ether (20 mL), two phases were separated. The aqueous phase was extracted with ether (2 × 20 mL). The combined organic layers were washed with saturated sodium bicarbonate (1 × 20 mL) and brine (1 × 20 mL) and dried over sodium sulfate. The crude compound was purified on silica gel eluted with 20% ethyl acetate in hexane to give (*S*)- or (*R*)-**4** as white solid. (*S*)-3-(*tert*-Butoxycarbonyl)-4-methyl-1,2,3-oxathiazolidine-4-carboxylic acid *tert*-butyl ester 2,2-dioxide ((*S*)-**4**), 139 mg (85.6%), mp 69−70 °C (ethyl acetate/hexane). ^{1}H NMR ($CDCl_3$), δ 1.50

(9H, s), 1.57 (9H, s), 1.74 (3H, s), 4.26, 4.29 (1H, d, J = 9.6 Hz), 4.56, 4.58 (1H, d, J = 9.6 Hz). HRMS, m/z, calcd for $C_{13}H_{27}N_2O_7S$ [M + NH_4]$^+$, 355.15335; found 355.15341 (100%). (*R*)-3-(*tert*-Butoxycarbonyl)-4-methyl-1,2,3-oxathiazolidine-4-carboxylic acid *tert*-butyl ester 2,2-dioxide ((*R*)-**4**), 138 mg (85.3%), mp 70−71 °C (ethyl acetate/hexane). ^{1}H NMR ($CDCl_3$), δ 1.50 (9H, s), 1.57 (9H, s), 1.74 (3H, s), 4.26, 4.29 (1H, d, J = 9.3 Hz), 4.56, 4.59 (1H, d, J = 9.3 Hz), Anal. ($C_{13}H_{23}NO_7S$) C, H, N.

(*R*)- and (*S*)-2-Amino-3-fluoro-2-methylpropanoic Acid (5), Hydrochloride Salt. Compounds (*R*)- and (*S*)-**5** were prepared from (*S*)- and (*R*)-**4**, respectively, using the method previously reported.[22] Briefly, to a solution of the cyclic sulfamidate (*S*)- or (*R*)-**4** (30 mg, 0.089 mmol) in 1 mL of acetonitrile was added tetrabutylammonium fluoride (71 mg, 0.27 mmol, 270 μL of 1.0 M solution in tetrahydrofuran), and the resulting solution was stirred overnight at room temperature. The reaction mixture was concentrated under reduced pressure, and the residue was treated with 5 mL of 3N hydrochloric acid at 85 °C for 1 h. After cooling, the aqueous solution was washed twice with 5 mL of ether and then concentrated under reduced pressure to give (*R*)- or (*S*)-**5**-HCl as white solid. (*R*)-2-Amino-3-fluoro-2-methylpropanoic acid, hydrochloride salt ((*R*)-**5**-HCl), 7 mg (49.9%), mp 204−206 °C (decomposed). ^{1}H NMR (D_2O) δ 1.50 (3H, s), 4.53−4.90 (2H, m). Anal. ($C_4H_9ClFNO_2$) C, H, N. (*S*)-2-Amino-3-fluoro-2-methylpropanoic acid, hydrochloride salt ((*S*)-**5**-HCl), 6.3 mg (44.9%), mp 202−205 °C (decomposed). ^{1}H NMR (D_2O) δ 1.52 (3H, s), 4.54−4.92 (2H, m). Anal. ($C_4H_9ClFNO_2$) C, H, N.

(*S*)- and (*R*)-4-Methyl-1,2,3-oxathiazolidine-4-carboxylic Acid *tert*-Butyl Ester 2,2-Dioxide (6). To a solution of (*S*)- or (*R*)-**4** (161 mg, 0.478 mmol) in 2 mL of *tert*-butyl acetate-dichloromethane (4:1 v/v) was added methanesulfonic acid (138 mg, 1.43 mmol) at room temperature under an argon atmosphere. After stirring at room temperature overnight, 5 mL of saturated sodium bicarbonate was added to the mixture. The aqueous phase was extracted with ethyl acetate (3 × 10 mL). The combined organic phases were washed with brine (1 × 10 mL), dried over sodium sulfate, and concentrated under reduced pressure. The crude product was purified with silica gel chromatography (20% ethyl acetate in hexane) to give **6** as colorless oil. (*S*)-4-Methyl-1,2,3-oxathiazolidine-4-carboxylic acid *tert*-butyl ester 2,2-dioxide ((*S*)-**6**), 64 mg (56.5%). ^{1}H NMR ($CDCl_3$) δ 1.53 (9H, s), 1.63 (3H, s), 4.27, 4.30 (1H, d, J = 9.6 Hz), 4.69, 4.72 (1H, d, J = 9.6 Hz), 5.51 (1H, broad s). Anal. ($C_8H_{15}NO_5S$) C, H, N. (*R*)-4-Methyl-1,2,3-oxathiazolidine-4-carboxylic acid *tert*-butyl ester 2,2-dioxide ((*R*)-**6**), 56.1 mg (49.5%). ^{1}H NMR ($CDCl_3$) δ 1.53 (9H, s), 1.63 (3H, s), 4.272, 4.30 (1H, d, J = 9.6 Hz), 4.69, 4.72 (1H, d, J = 9.6 Hz), 5.49 (1H, broad s). Anal. ($C_8H_{15}NO_5S$) Calcd C: 40.50, H: 6.37, N: 5.90. Found C: 41.08, H: 6.41, N: 5.78.

(*S*)- and (*R*)-3,4-Dimethyl-1,2,3-oxathiazolidine-4-carboxylic Acid *tert*-Butyl Ester 2,2-Dioxide (7). To a solution of (*S*)- or (*R*)-**6** (22 mg, 0.093 mmol) in 1 mL of tetrahydrofuran was added sodium hydride (9 mg, 0.37 mmol) at room temperature under an argon atmosphere and the mixture was stirred for 10 min after which dimethyl sulfate (47 mg, 0.37 mmol) was added dropwise. The mixture was stirred at room temperature overnight. Water (2 mL) was added, and the mixture was extracted with ethyl acetate (2 × 5 mL). The combined organic phases were dried over sodium sulfate and concentrated under reduced pressure. The crude product was purified by silica gel column eluted with 20% ethyl acetate in hexane to give the title compound as white solid. (*S*)-3,4-Dimethyl-1,2,3-oxathiazolidine-4-carboxylic acid *tert*-butyl ester 2,2-dioxide ((*S*)-**7**), 13.3 mg (56.9%), mp 84−85 °C (ethyl acetate/hexane). ^{1}H NMR ($CDCl_3$) δ 1.51 (9H, s), 1.53 (3H, s), 2.94 (3H, s), 4.22, 4.24 (1H, d, J = 8.4 Hz), 4.88, 4.90 (1H, d, J = 8.4 Hz). Anal. ($C_9H_{17}NO_5S$) C, H, N. (*R*)-3,4-Dimethyl-1,2,3-oxathiazolidine-4-carboxylic acid *tert*-butyl ester 2,2-dioxide ((*R*)-**7**), 15.5 mg (66.4%), mp 84−85 °C (ethyl acetate /hexane). ^{1}H NMR ($CDCl_3$) δ 1.51 (9H, s), 1.53 (3H, s), 2.94 (3H, s), 4.21, 4.24 (1H, d, J = 8.7 Hz), 4.88, 4.91 (1H, d, J = 8.7 Hz). Anal. ($C_9H_{17}NO_5S$) C, H, N.

(*R*)- and (*S*)-3-Fluoro-2-methyl-2-(methylamino)propanoic Acid (8), Hydrochloride Salt. (*R*)- and (*S*)-**8** were prepared from (*S*)- and (*R*)-**7**, respectively. To a solution of the cyclic sulfamidate (*S*)- or (*R*)-**7** (16 mg, 0.06 mmol) in 1 mL of acetonitrile was added tetrabutylammonium fluoride (47 mg, 0.18 mmol, 180 μL of 1.0 M solution in tetrahydrofuran), and the resulting solution was stirred overnight at room temperature. The reaction mixture was concentrated under reduced pressure, and the residue was treated with 5 mL of 3N hydrochloric acid at 85 °C for 1 h. After cooling, the aqueous solution was washed twice with 5 mL of ether and then concentrated under reduced pressure to give (*R*)- or (*S*)-**8**-HCl as white solid. (*R*)-3-fluoro-2-methyl-2-(methylamino)propanoic acid, hydrochloride salt ((*R*)-**8**-HCl), 5 mg (49%), mp 179−181 °C (decomposed). ^{1}H NMR (D_2O) δ 1.47−1.48 (3H, m), 2.73 (3H, s), 4.64−4.90 (2H, m). Anal. ($C_5H_{11}ClFNO_2$) C, H, N. (*S*)-3-Ffluoro-2-methyl-2-(methylamino)propanoic acid, hydrochloride salt ((*S*)-**8**-HCl), 4.1 mg (40%), mp 178−181 °C (decomposed). ^{1}H NMR (D_2O) δ 1.47−1.49 (3H, m), 2.75 (3H, s), 4.65−4.92 (2H, m). Anal. ($C_5H_{11}ClFNO_2$) C, H, N.

Radiosynthesis of (*R*)- and (*S*)-2-Amino-3-[^{18}F]fluoro-2-methylpropanoic Acid ((*R*)- and (*S*)-[^{18}F]5) and (*R*)- and (*S*)-3-[^{18}F]Fluoro-2-methyl-2-(methylamino)propanoic Acid ((*R*)- and (*S*)-[^{18}F]8). The same conditions were used to prepare FAMP (*R*)-[^{18}F]**5** from (*S*)-**4**, (*S*)-[^{18}F]**5** from (*R*)-**4**, *N*Me-FAMP (*R*)-[^{18}F]**8** from (*S*)-**7**, and (*S*)-[^{18}F]**8** from (*R*)-**7**, respectively. The preparation of (*R*)- and (*S*)-[^{18}F]**5** as well as (*R*)- and (*S*)-[^{18}F]**8** was based on the previously reported automated synthesis of *anti*-[^{18}F]FACBC, which involved a fully automated synthesis developed for the Siemens computer programmable chemistry process control unit (CPCU).[31] The CPCU is a valve-and-tubing system which is designed to accommodate one or two glass reaction vessels and a number of reagent and solvent reservoir containers. The automated production of the ^{18}F-labeled amino acids was started by delivering 150−200 mCi NCA [^{18}F]HF from cyclotron target through a trap/release cartridge T/R by using 0.9 mg (6.5 μmol) potassium carbonate in 0.6 mL of water to a reaction vial containing 5 mg (13.3 μmol) of Kryptofix 222 in 1 mL of acetonitrile. The solvent was removed at 110 °C with nitrogen gas flow. Acetonitrile (1 mL) was added, and the drying was repeated three times to remove residual water. A 1 mg portion of the appropriate cyclic sulfamidate **4** or **7** in 1 mL of acetonitrile was added to the vial, and the reaction mixture was heated at 90 °C for 10 min. After acidic hydrolysis using 0.5 mL of 4N hydrochloric acid at 110 °C for 10 min, the product was purified[47] by passing serially through an AG 11A8 ion retardation resin column, an alumina N SepPak, an HLB Oasis reverse phase cartridge, and a 0.2 μm Gelman Teflon filter with sterile normal saline into a dose vial, which was ready for use in vitro and in vivo studies. The identity of the radiolabeled product was confirmed by comparing the R_f value of the radioactive product visualized with radiometric TLC with the R_f value of the authentic ^{19}F compound visualized with ninhydrin stain, with a solvent of acetonitrile/water/methanol = 4:1:1 (v/v/v) (R_f = 0.4 for **5**, R_f = 0.5 for **8**). In all radiosyntheses, the only peak present on radiometric TLC analysis corresponded to **5** or **8**, and the radiochemical purity of the product exceeded 99%.

Amino Acid Uptake and Inhibition Assays. These assays were performed by a modified reported method,[22,38] and the procedures are summarized here. The 9L rat gliosarcoma cell line was cultured in Dulbecco's Modified Eagle's Medium (DMEM) supplemented with 10% fetal calf serum, 100 units/mL penicillin, and 100ug/mL streptomycin. Cells were maintained in T-150 tissue culture flasks under humidified incubator conditions (37 °C, 5% CO_2/95% air) and were routinely passaged at confluence. For the cell uptake experiment, 9L cells were

dispersed with a 0.05% solution of trypsin/ethylenediaminetetraacetic acid (EDTA), washed with Hank's balanced salt solution (HBSS) twice, and adjusted to a final concentration of 5×10^7 cells/mL in HBSS.

In this study, approximately 5×10^5 cells were exposed to 5 μCi (*R*)-[^{18}F]**5**, (*S*)-[^{18}F]**5**, (*R*)- [^{18}F]**8**, or (*S*)-[^{18}F]**8** in amino acid free HBSS (0.1 mL) with or without transport inhibitors (10 mM final concentration of BCH, MeAIB or ACS, respectively) for 30 min under incubator conditions in 1.5 mL conical tubes. Each assay condition was performed in triplicates. After incubation, cells were twice centrifuged (75 G for 5 min) and rinsed with ice-cold amino-acid/serum-free HBSS to remove residual activity in the supernatant. The activity in tubes was counted in a Packard Cobra II Auto-Gamma counter, the raw counts decay corrected, and the activity per cell number determined. The data from these studies (expressed and normalized as percent uptake relative to control per 5×10^5 cells) were graphed using Excel, with statistical comparisons using 1-way ANOVA with ProStat software (Poly Software International, Pearl River, NY) between the groups analyzed.

Tumor Induction and Animal Preparation. Rat 9L gliosarcoma cells for intracranial implantation experiments were cultured and prepared the same way as the uptake and inhibition assays and then were washed with phosphate buffer solution (PBS) and were made a final concentration of $5 \times 10^4/5$ μL in PBS. Rat 9L gliosarcoma cells were implanted into the brains of male Fischer 344 rats (200−250 g) as described previously.[19,22,38] Briefly, following anesthesia with an intramuscular injection of ketamine (60 mg/mL) and xylazine (7.5 mg/mL) solution, rats were placed in a stereotactic head holder and were injected with 5 μL suspension of rat 9L gliosarcoma cells (5×10^4 cells per rat) in a location 3 mm right of midline and 1 mm anterior to the bregma at 4 mm deep to the outer table. The injection was performed over the course of 2 min, and the needle was withdrawn over the course of 1 min to minimize the backflow of tumor cells. The burr hole and scalp incision were closed, and the animals were returned to their original cages after recovering from the procedure. Intracranial tumors developed that produced weight loss, apathy, and hunched posture in the tumor-bearing rats. Typically, among 25 animals implanted with tumor cells, 20 would develop tumors visible to the naked eye upon dissection in approximately 10−12 days and were used in the study.

Rodent Biodistribution Studies. The tissue distribution of radioactivity was measured in 16−20 tumor-bearing rats, which had been implanted with 9L cells for 10−12 days and were allowed food and water ad libitum before the experiment. The rats were anesthetized using a mixture of 2:1 ketamine (100 mg/mL):xylazine (20 mg/mL). Dose of anesthesia was 0.16 mL/100 g of rat. This provided 1.5−2 h of anesthesia for purpose of catheter placement and injection of radiotracer compound. A 24 gauge × 0.75 in. catheter was placed in one of lateral tail veins of the anesthetized rat. This facilitated the later injection of radiotracer. Rats were injected in groups of 4−5 rats per group. The animals were injected of approximately 20 μCi of radiotracer (*R*)-[^{18}F]**5**, (*S*)-[^{18}F]**5,** (*R*)-[^{18}F]**8**, or (*S*)-[^{18}F]**8** in 0.5 mL of sterile normal saline via catheters into tail veins. The groups of rats were sacrificed at 30, 60, and 120 min, respectively, post injection for (*R*)- and (*S*)-[^{18}F]**5** and at 15, 30, 60, and 120 min respectively, post injection for (*R*)- and (*S*)-[^{18}F]**8**. Euthanasia was achieved by injection of a saturated solution of potassium chloride into the heart of animals while under anesthesia. The animals were dissected; tumors and selected tissues were weighed and the activity counted along with dose standards in a Packard Cobra II Auto-Gamma counter. The raw counts were decay corrected, and the counts were normalized as the percent of total injected dose per gram of tissue (%ID/g). The uptake in tumor and normal brain was compared at each time point for the each enantiomer pair using 1-way ANOVA corrected for multiple comparisons with ProStat software. The differences in uptake between normal tissues were compared at each time point for each tracer using 1-way ANOVA with ProStat software.

Acknowledgment. We are grateful to Dr. Bing Wang, NMR Center of Emory University, for the help with NMR instrumentation, sample treatment, and data analysis. We acknowledge the use of Shared Instrumentation provided by grants from the NIH and the NMP for the mass spectrometry data.

References

(1) Conti, P. S.; Lilien, D. L.; Hawley, K.; Keppler, J.; Grafton, S. T.; Bading, J. R. PET and [^{18}F]-FDG in oncology: a clinical update. *Nucl. Med. Biol.* **1996**, *23* (6), 717–735.
(2) Kelloff, G. J.; Hoffman, J. M.; Johnson, B.; Scher, H. I.; Siegel, B. A.; Cheng, E. Y.; Cheson, B. D.; O'Shaughnessy, J.; Guyton, K. Z.; Mankoff, D. A.; Shankar, L.; Larson, S. M.; Sigman, C. C.; Schilsky, R. L.; Sullivan, D. C. Progress and Promise of FDG-PET Imaging for Cancer Patient Management and Oncologic Drug Development. *Clin. Cancer Res.* **2005**, *11*, 2785–2808.
(3) Barentsz, J.; Takahashi, S.; Oyen, W. M., R.; De Mulder, P.; Reznek, R.; Oudkerk, M.; Mali, W. Commonly Used Imaging Techniques for Diagnosis and Staging. *J. Clin. Oncol.* **2006**, *24* (20), 3234–3244.
(4) Pauwels, E. K. J.; Ribeiro, M. J.; Stoot, J. H. M. B.; McCready, V. R.; Bourguignon, M.; Mazière, B. FDG Accumulation and Tumor Biology. *Nucl. Med. Biol.* **1998**, *25* (4), 317–322.
(5) Jager, P. L.; Vaalburg, W.; Pruim, J.; de Vries, E. G.; Langen, K. J.; Piers, D. A. Radiolabeled Amino Acids: Basic Aspects and Clinical Applications in Oncology. *J. Nucl. Med.* **2001**, *42*, 432–445.
(6) Laverman, P.; Boerman, O. C.; Corstens, F. H.; Oyen, W. J. Fluorinated amino acids for tumour imaging with positron emission tomography. *Eur. J. Nucl. Med.* **2002**, *29*, 681–690.
(7) Grosu, A. L.; Weber, W. A.; Franz, M.; Staerk, S.; Piert, M.; Thamm, R.; Gumprecht, H.; Schwaiger, M.; Molls, M.; Nieder, C. Reirradiation of recurrent high-grade gliomas using amino acid PET (SPECT)/CT/MRI image fusion to determine gross tumor volume for stereotactic fractionated radiotherapy. *Int. J. Radiat. Oncol., Biol., Phys.* **2005**, *63* (2), 511–519.
(8) Jager, P. L. Improving Amino Acid Imaging: Hungry or Stuffed? *J. Nucl. Med.* **2002**, *43* (9), 1207–1209.
(9) McConathy, J.; Goodman, M. M. Non-natural amino acids for tumor imaging using positron emission tomography and single photon emission computed tomography. *Cancer Metastasis Rev.* **2008**, *27*, 555–573.
(10) Fuchs, B. C.; Bode, B. P. Amino acid transporters ASCT2 and LAT1 in cancer: Partners in crime? *Semin. Cancer Biol.* **2005**, *15* (4), 254–266.
(11) Fuchs, B. C.; Finger, R. E.; Onan, M. C.; Bode, B. P. ASCT2 silencing regulates mammalian target-of-rapamycin growth and survival signaling in human hepatoma cells. *Am. J. Physiol.: Cell Physiol.* **2007**, *293* (1), C55–63.
(12) Johnstone, R. M.; Scholefield, P. G. Amino acid transport in tumor cells. *Adv. Cancer Res.* **1965**, *9*, 143–226.
(13) Langen, K. J.; Hamacher, K.; Weckesser, M.; Floeth, F.; Stoffels, G.; Bauer, D.; Coenen, H. H.; Pauleit, D. *O*-(2-[^{18}F]fluoroethyl)-L-tyrosine: uptake mechanisms and clinical applications. *Nucl. Med. Biol.* **2006**, *33*, 287–294.
(14) Biersack, H. J.; Coenen, H. H.; Stocklin, G.; Reichmann, K.; Bockisch, A.; Oehr, P.; Kashab, M.; Rollmann, O. Imaging of brain tumors with L-3-[^{123}I]iodo-α-methyl tyrosine and SPECT. *J. Nucl. Med.* **1989**, *30* (1), 110–112.
(15) Langen, K. J.; Coenen, H. H.; Roosen, N.; Kling, P.; Muzik, O.; Herzog, H.; Kuwert, T.; Stocklin, G.; Feinendegen, L. E. SPECT studies of brain tumors with L-3-[^{123}I]iodo-α-methyl tyrosine: comparison with PET, ^{124}IMT and first clinical results. *J. Nucl. Med.* **1990**, *31*, 281–286.
(16) Langen, K. J.; Pauleit, D.; Coenen, H. H. 3-[^{123}I]Iodo-α-methyl-L-tyrosine: uptake mechanisms and clinical applications. *Nucl. Med. Biol.* **2002**, *29*, 625–631.
(17) Gulyas, B.; Nyary, I.; Borbely, K. FDG, MET or CHO? The quest for the optimal PET tracer for glioma imaging continues. *Nature Clin. Pract. Neurol.* **2008**, *4* (9), 470–471.
(18) Lilja, A.; Bergstrom, K.; Hartvig, P.; Spannare, B.; Halldin, C.; Lundqvist, H.; Langstrom, B. Dynamic study of supratentorial gliomas with L-methyl-^{11}C-methionine and positron emission tomography. *Am. J. Neuroradiol.* **1985**, *6* (4), 505–514.
(19) Shoup, T. M.; Olson, J.; Hoffman, J. M.; Votaw, J.; Eshima, D.; Eshima, L.; Camp, V. M.; Stabin, M.; Votaw, D.; Goodman, M. M.

Synthesis and Evaluation of [^{18}F]1-Amino-3-Fluorocyclobutane-1-Carboxylic Acid to Image Brain Tumors. *J. Nucl. Med.* **1999**, *40*, 331–338.

(20) Schmall, B.; Conti, P. S.; Bigler, R. E.; Zanzonico, P. B.; Dahl, J. R.; Sundoro-Wu, B. M.; Jacobsen, J. K.; Lee, R. Synthesis and quality assurance of [^{11}C]alpha-aminoisobutyric acid (AIB), a potential radiotracer for imaging and amino acid transport studies in normal and malignant tissues. *Int.J. Nucl. Med. Biol.* **1984**, *11* (3/4), 209–214.

(21) Sutinen, E.; Jyrkkio, S.; Gronroos, T.; Haaparanta, M.; Lehikoinen, P.; Nagren, K. Biodistribution of [^{11}C]methylaminoisobutyric acid, a tracer for PET studies on system A amino acid transport in vivo. *Eur. J. Nucl. Med.* **2001**, *28* (7), 847–854.

(22) McConathy, J.; Martarello, L.; Malveaux, E. J.; Camp, V. M.; Simpson, N. E.; Simpson, C. P.; Bowers, G. D.; Olson, J. J.; Goodman, M. M. Radiolabeled amino acids for tumor imaging with PET: radiosynthesis and biological evaluation of 2-amino-3-[^{18}F]fluoro-2-methylpropanoic acid and 3-[^{18}F]fluoro-2-methyl-2-(methylamino)propanoic acid. *J. Med. Chem.* **2002**, *45*, 2240–2249.

(23) Yu, W.; McConathy, J.; Olson, J. J.; Camp, V. M.; Goodman, M. M. Facile Stereospecific Synthesis and Biological Evaluation of (*S*)- and (*R*)-2-Amino-2-methyl-4-[^{123}I]iodo-3-(*E*)-butenoic Acid for Brain Tumor Imaging with Single Photon Emission Computerized Tomography. *J. Med. Chem.* **2007**, *50*, 6718–6721.

(24) Ludwig, J.; Lehr, M. Convenient Synthesis of Pyrrole- and Indolecarboxylic Acid *tert*-Butylesters. *Synth. Commun.* **2004**, *34* (20), 3691–3695.

(25) Widmer, U. A convenient preparation of *t*-butyl esters. *Synthesis* **1983**, 135–136.

(26) Dutta, A. K.; Xu, C.; Reith, M. E. A. Structure−activity relationship studies of novel 4-[2-[bis(4-fluorophenyl)methoxy]ethyl]-1-(3-phenylpropyl)piperidine analogs: synthesis and biological evaluation at the dopamine and serotonin transporter sites. *J. Med. Chem.* **1996**, *39*, 749–756.

(27) Posakony, J. J.; Grierson, J. R.; Tewson, T. J. New routes to *N*-alkylated cyclic sulfamidates. *J. Org. Chem.* **2002**, *67*, 5164–5169.

(28) Han, G.; Tamaki, M.; Hruby, V. J. Fast, efficient and selective deprotection of the *tert*-butoxycarbonyl (Boc) group using HCl/dioxane (4 M). *J. Pept. Res.* **2001**, *58* (4), 338–341.

(29) Lin, L. S.; Lanza, T.; de Laszlo, S. E.; Truong, Q.; Kamenecka, T.; Hagmann, W. K. Deprotection of *N*-*tert*-butoxycarbonyl (Boc) groups in the presence of *tert*-butyl esters. *Tetrahedron Lett.* **2000**, *41* (36), 7013–7016.

(30) Prashad, M.; Har, D.; Hu, B.; Kim, H.-Y.; Repic, O.; Blacklock, T. J. An Efficient and Practical *N*-Methylation of Amino Acid Derivatives. *Org. Lett.* **2003**, *5* (2), 125–128.

(31) McConathy, J.; Voll, R. J.; Yu, W.; Crowe, R. J.; Goodman, M. M. Improved synthesis of *anti*-[^{18}F]FACBC: improved preparation of labeling precursor and automated Radiosynthesis. *Appl. Radiat. Isot.* **2003**, *58*, 657–666.

(32) Alexoff, D. L.; Casati, R.; Fowler, J. S.; Wolf, A. P.; Shea, C.; Schlyer, D. J.; Shiue, C. Y. Ion chromatographic analysis of high specific activity ^{18}FDG preparations and detection of the chemical impurity 2-deoxy-2-chloro-D-glucose. *Int. J. Radiat. Appl. Instr., Part A* **1992**, *43*, 1313–1322.

(33) Christensen, H. N. Role of amino acid transport and countertransport in nutrition and metabolism. *Physiol. Rev.* **1990**, *70* (1), 43–77.

(34) Souba, W. W.; Pacitti, A. J. How amino acids get into cells: mechanisms, models, menus, and mediators. *JPEN, J. Parenter. Enteral Nutr.* **1992**, *16* (6), 569–78.

(35) Palacin, M.; Estevez, R.; Bertran, J.; Zorzano, A. Molecular biology of mammalian plasma membrane amino acid transporters. *Physiol. Rev.* **1998**, *78*, 969–1054.

(36) Saier, M. H. J.; Daniels, G. A.; Boerner, P.; Lin, J. Neutral amino acid transport systems in animal cells: potential targets of oncogene action and regulators of cellular growth. *J. Membr. Biol.* **1988**, *104*, 1–20.

(37) Shotwell, M. A.; Kilberg, M. S.; Oxender, D. L. The regulation of neutral amino acid transport in mammalian cells. *Biochim. Biophys. Acta, Rev. Biomembr.* **1983**, *737*, 267–284.

(38) Martarello, L.; McConathy, J.; Camp, V. M.; Malveaux, E. J.; Simpson, N. E.; Simpson, C. P.; Olson, J. J.; Bowers, G. D.; Goodman, M. M. Synthesis of *syn*- and *anti*-1-amino-3-[^{18}F]fluoromethyl-cyclobutane-1-carboxylic acid (FMACBC), potential PET ligands for tumor detection. *J. Med. Chem.* **2002**, *45*, 2250–2259.

(39) McConathy, J.; Martarello, L.; Malveaux, E. J.; Camp, V. M.; Simpson, N. E.; Simpson, C. P.; Bowers, G. D.; Zhang, Z.; Olson, J. J.; Goodman, M. M. Synthesis and evaluation of 2-amino-4-[^{18}F]fluoro-2-methylbutanoic acid (FAMB): relationship of amino acid transport to tumor imaging properties of branched fluorinated amino acids. *Nucl. Med. Biol.* **2003**, *30*, 477–490.

(40) Conti, P. S.; Sordillo, E. M.; Sordillo, P. P.; Schmall, B. Tumor localization of alpha-aminoisobutyric acid (AIB) in human melanoma heterotransplants. *Eur. J. Nucl. Med.* **1985**, *10* (1−2), 45–47.

(41) Dunzendorfer, U.; Schmall, B.; Bigler, R. E.; Zanzonico, P. B.; Conti, P. S.; Dahl, J. R.; Kleinert, E.; Whitmore, W. F. Synthesis and body distribution of alpha-aminoisobutyric acid-L-^{11}C in normal and prostate cancer-bearing rat after chemotheraphy. *Eur. J. Nucl. Med.* **1981**, *6*, 535–538.

(42) Heiss, P.; Mayer, S.; Herz, M.; Wester, H. J.; Schwaiger, M.; Senekowitsch-Schmidtke, R. Investigation of transport mechanism and uptake kinetics of *O*-(2-[^{18}F]fluoroethyl)-L-tyrosine in vitro and in vivo. *J. Nucl. Med.* **1999**, *40*, 1367–1373.

(43) Kersemans, V.; Cornelissen, B.; Kersemans, K.; Bauwens, M.; Achten, E.; Dierckx, R. A.; Mertens, J.; Slegers, G. In vivo characterization of ^{123}/^{125}I-2-iodo-L-phenylalanine in an R1M rhabdomyosarcoma athymic mouse model as a potential tumor tracer for SPECT. *J. Nucl. Med.* **2005**, *46* (3), 532–539.

(44) Lahoutte, T.; Mertens, J.; Caveliers, V.; Franken, P. R.; Everaert, H.; Bossuyt, A. Comparative biodistribution of iodinated amino acids in rats: selection of the optimal analog for oncologic imaging outside the brain. *J. Nucl. Med.* **2003**, *44*, 1489–1494.

(45) Samnick, S.; Schaefer, A.; Siebert, S.; Richter, S.; Vollmar, B.; Kirsch, C. M. Preparation and investigation of tumor affinity, uptake kinetic and transport mechanism of iodine-123-labelled amino acid derivatives in human pancreatic carcinoma and glioblastoma cells. *Nucl. Med. Biol.* **2001**, *28*, 13–23.

(46) Wester, H. J.; Herz, M.; Weber, W.; Heiss, P.; Senekowitsch-Schmidtke, R.; Schwaiger, M.; Stocklin, G. Synthesis and radiopharmacology of *O*-(2-^{18}F-fluoroethyl)-L-tyrosine for tumor imaging. *J. Nucl. Med.* **1999**, *40*, 205–212.

(47) Yu, W.; Williams, L.; Camp, V. M.; Malveaux, E.; Olson, J. J.; Goodman, M. M. Stereoselective synthesis and biological evaluation of *syn*-1-amino-3-[^{18}F]-fluorocyclobutyl-1-carboxylic acid as a potential positron emission tomography brain tumor imaging agent. *Bioorg. Med. Chem.* **2009**, *17*, 1982–1990.